

NCAT Report 15-05R

**REFINED LIMITING STRAIN CRITERIA AND
APPROXIMATE RANGES OF MAXIMUM
THICKNESSES FOR DESIGNING LONG-LIFE
ASPHALT PAVEMENTS**

(First Revision)

By

**Dr. Nam Tran, P.E.
Dr. Mary M. Robbins
Dr. David H. Timm, P.E.
Dr. J. Richard Willis
Dr. Carolina Rodezno**

November 2016



**National Center for
Asphalt Technology**
NCAT
at AUBURN UNIVERSITY

277 Technology Parkway ■ Auburn, AL 36830

**Refined Limiting Strain Criteria and Approximate Ranges of Maximum Thicknesses for
Designing Long-Life Asphalt Pavements**

Dr. Nam Tran, P.E.
Associate Research Professor
National Center for Asphalt Technology

Dr. Mary M. Robbins
Assistant Research Professor
National Center for Asphalt Technology

Dr. David H. Timm, P.E.
Brasfield and Gorrie Professor of Civil Engineering
Principal Investigator

Dr. J. Richard Willis
Associate Research Professor
National Center for Asphalt Technology

Dr. Carolina Rodezno
Assistant Research Professor
National Center for Asphalt Technology

Sponsored by
National Asphalt Pavement Association

November 2016

ACKNOWLEDGEMENTS

The authors wish to thank the National Asphalt Pavement Association for sponsoring this research as part of the Optimizing Flexible Pavement Design and Material Selection research project and for providing technical review of this document.

DISCLAIMER

The contents of this report reflect the views of the authors who are responsible for the facts and accuracy of the data presented herein. The contents do not necessarily reflect the official views or policies of the National Center for Asphalt Technology or Auburn University. This report does not constitute a standard, specification, or regulation. Comments contained in this paper related to specific testing equipment and materials should not be considered an endorsement of any commercial product or service; no such endorsement is intended or implied.

NOTES ON FIRST REVISIONS

NCAT Report 15-05 was revised in November 2016 to address errors found in Tables 13, 14, and 15.

TABLE OF CONTENTS

- 1 Introduction 5
- 2 Review of Design Thresholds and Thickness Requirements..... 6
 - 2.1 Bottom-Up Fatigue Cracking 6
 - 2.2 Structural Rutting 9
 - 2.3 Pavement Thicknesses 10
- 3 Evaluation and Refinement of Design Thresholds..... 11
 - 3.1 Fatigue Endurance Limit as Design Threshold 11
 - 3.2 Cumulative Strain Distribution as Design Threshold 13
 - 3.3 Refining Design Thresholds for Perpetual Pavement Design 15
 - 3.3.1 Pavement Sections and Field Performance 16
 - 3.3.2 Field Performance 19
 - 3.3.3 Analysis Methodology 20
 - 3.3.4 Refined Limiting Strain Criteria for Use in Perpetual Pavement Design..... 25
 - 3.3.5 Validating Refined Design Thresholds 27
- 4 Approximate Ranges of Maximum Design Thicknesses 29
- 5 Conclusions 34
- 6 Recommendations 36
- 7 References..... 37

1 INTRODUCTION

Many transportation agencies are currently conducting the design and analysis of asphalt pavements based on the 1993 (or earlier) version of American Association of State Highway and Transportation Officials (AASHTO) Guide for Design of Pavement Structures (0). These empirical design procedures were developed based on the data collected during the AASHTO Road Test conducted from 1958 through 1961 (2).

Due to limited testing conditions included in the AASHTO Road Test experiment and significant changes in traffic loads and materials over the years, pavement designs today are often based on extrapolation far beyond the experimental conditions. One consequence of this extrapolation is ever-increasing thickness with traffic volume, resulting in overly designed asphalt pavements for high volume roadways (3). This raises the concern over the accuracy and effectiveness of these procedures for designing heavily trafficked pavements.

To address the limitation in the empirical design procedures, the Asphalt Pavement Alliance (APA) introduced the concept of Perpetual Pavements in 2000 (3). As illustrated in Figure 1, a perpetual pavement is designed to have appropriate layer thicknesses and materials for addressing specific pavement distresses, especially those causing structural damage that initiates at the bottom of the pavement. To avoid these structural distresses, including bottom-up fatigue cracking and subgrade rutting, the pavement's responses, such as stresses, strains, and displacements, must be lower than thresholds at which structural distresses begin to occur. Thus, the design can be optimized to sustain the heaviest loads without additional structure, providing an indefinite structural life without being overly conservative (3). An asphalt pavement that is built properly and designed according to this concept should last longer than 50 years without a major rehabilitation or reconstruction and would just need periodic resurfacing to remedy surface distresses (4).

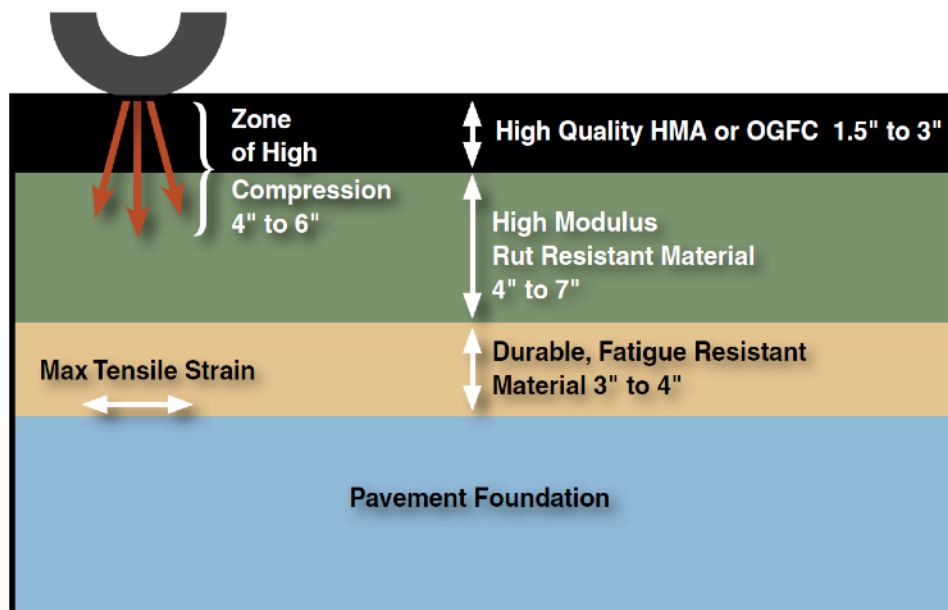


Figure 1 Perpetual Pavement Design Concept (3).

Currently, most approaches to perpetual pavement design focus on preventing bottom-up fatigue cracking and subgrade rutting from occurring at the bottom of the pavement structure (3). One method of reducing these critical structural distresses is to increase the pavement thicknesses to ensure that critical pavement responses are well below design thresholds. In doing so, however, it is important to recognize that maximum thicknesses may exist such that additional material is not necessary in prolonging the structural life of a pavement. For example, in their investigation of long-life pavements in the United Kingdom (UK), Nunn and Ferne (5) reported that a conservative asphalt layer thickness of 15.4 inches was sufficient for long-life asphalt pavements. This thickness included 10.6 inches of asphalt to prevent bottom-up fatigue cracking, 4 inches of asphalt to mitigate top-down cracking (top-down cracks were seen to propagate up to 4 inches from the surface at the time of resurfacing) and an additional 0.8 inches to account for an increase in the legal load limit in the UK. As a result, no additional thickness beyond 15.4 inches was necessary to ensure long life.

The objective of this study was to determine critical pavement design thresholds and approximate ranges of maximum thicknesses for flexible pavements in an effort to improve the cost effectiveness of long-life asphalt pavements. This study was divided into two tasks. The first task was to review literature pertaining to design thresholds and maximum thickness requirements for perpetual pavements. The second task was to establish design thresholds and approximate ranges of maximum pavement thicknesses using the information reviewed in Task 1 and through analyzing information from the fully instrumented pavement sections at the NCAT Pavement Test Track. This report summarizes the key findings of the two tasks and provides recommendations for implementing design thresholds and approximate ranges of maximum thickness for consideration in future pavement design.

2 REVIEW OF DESIGN THRESHOLDS AND THICKNESS REQUIREMENTS

A perpetual pavement is designed to resist structural distresses that initiate deep in the pavement structure and eventually require full-depth rehabilitation. The structural distresses included in most perpetual pavement design approaches are bottom-up fatigue cracking and subgrade rutting (3). To avoid these distresses, an appropriate asphalt pavement structure can be designed so that the horizontal tensile strains at the bottom of the asphalt layer and the vertical compressive strains and/or stresses at the top of the subgrade are lower than design thresholds below which structural damage does not initiate. Also, any additional pavement thickness than what is required to keep the critical strains/stresses below the design thresholds would not provide additional pavement service life. Different perpetual pavement design thresholds have been proposed over the past 20 years. A summary of these design thresholds and layer thickness requirements for designing perpetual pavements follows.

2.1 Bottom-Up Fatigue Cracking

Bottom-up fatigue cracking, also known as alligator cracking, severely affects a pavement's structural capacity. Figures 2 and 3 illustrate examples of fatigue cracking from the NCAT Pavement Test Track. These cracks typically form in the wheelpaths and initiate at the bottom of the asphalt concrete (AC) layer and propagate to the pavement surface due to repeated tensile strain events. Once cracks appear at the surface and water enters the pavement through

the cracks, further deterioration progresses quickly and reduces the strength of the underlying materials. The strength of the AC layer is also compromised by the presence of the cracks themselves. This form of distress is generally remedied by full-depth rehabilitation.



Figure 2 Examples of Bottom-Up Fatigue Cracking Observed at Pavement Surface.



Figure 3 Example of Bottom-Up Fatigue Cracking Observed in Cross-Section.

In a perpetual pavement design, the strains at the bottom of the asphalt structure are kept below a design strain threshold to prevent the initiation of bottom-up fatigue cracking. This design threshold is often the fatigue endurance limit (FEL) of the asphalt mixture used in the AC base layer. Thompson and Carpenter (6) described the FEL as representing the balance point between damage and healing while Bonaquist (7) described the FEL as, “A level of strain below which there is no cumulative damage over an indefinite number of load cycles.” Regardless of

the definition, bottom-up fatigue cracking is not expected to initiate in a pavement designed below the FEL.

Fatigue endurance limits may be determined through either laboratory testing by conducting bending beam fatigue tests (BBFT), or through field evaluation of existing pavements. One of the challenges, much like conventional BBFT testing to determine fatigue cracking transfer functions, is bridging the gap between laboratory test results and actual field performance.

An endurance limit of 70 microstrain was first reported for asphalt pavements by Monismith and McLean (8). Thompson and Carpenter reported in 2006 (6) that 70 microstrain should be considered the minimum value, as no lab data were found below this FEL, and a practical range is 70 to 100 microstrain. In 2009, Thompson and Carpenter (9) further stated, "A very conservative FEL is 70 microstrain. Laboratory studies have demonstrated that most HMA's display FELs well in excess of 70 microstrain." In support of this statement, Prowell et al. (10) provided laboratory testing data supporting the existence of a higher endurance limit that varied from 75 to 200 microstrain.

Laboratory testing conducted at the University of Illinois evaluating 120 different mixtures found FELs to vary from 90 to 300 microstrain (11). The FEL was found to depend on binder type and mixture composition (11). Furthermore, while mixture composition (i.e., volumetric parameters) was found to be important to the FEL, the gradation seemed to have relatively little effect on the FEL (11).

Fatigue endurance limits were also determined based on the analysis of long-life asphalt pavements. Nishizawa et al. (12) reported an endurance limit of 200 microstrain for in-service pavements in Japan. For a long-life pavement in Kansas, strain levels at the bottom of the asphalt layer were between 96 and 158 microstrain calculated from backcalculated stiffness data (13). Yang et al. (14) reported a successful perpetual pavement design in China using an endurance limit of 125 microstrain instead of a more conservative limit of 70 microstrain.

Von Quintus (15) examined pavement sections in the Long-Term Pavement Performance (LTPP) database to determine strain levels that correlated to less than a 2% chance of having fatigue cracking. He found 65 microstrain to yield a 95% confidence that cracking would not occur.

Based on full-scale pavement testing results at the NCAT Pavement Test Track, Willis and Timm (16) showed that asphalt pavements could withstand tensile strains greater than 100 microstrain at the bottom of the asphalt layer. They proposed a profile of limiting strains at the bottom of the asphalt layer that was found to distinguish the field performance of test sections better than one design endurance limit used in the past. The limiting strains were divided by the laboratory endurance limit to determine the maximum fatigue ratios as shown in Table 1. This method is detailed later in this report.

It is important to understand that the fatigue ratios in Table 1 were based on field-measured strain levels at the NCAT Pavement Test Track. While accurate, it is not practical to frequently instrument pavements for design purposes, and fatigue ratios based on simulated strain levels is desirable. Therefore, as presented later in this report, it was necessary to establish critical fatigue ratio levels based on simulated strain levels through mechanistic simulation software.

Table 1 Maximum Fatigue Ratios Based on Measured Strain (16)

Percentile	Maximum Fatigue Ratio
99%	2.83
95%	2.45
90%	2.18
85%	1.98
80%	1.85
75%	1.74
70%	1.63
65%	1.53
60%	1.44
55%	1.35
50%	1.27

2.2 Structural Rutting

Structural rutting occurs in the aggregate base, subgrade layer, or both, under the imposed traffic. Figure 4 illustrates rutting that is occurring in the base and subgrade layers where distortion of these layers mirrors a rut in the surface. To control structural rutting in a perpetual pavement design, the vertical strain or stress at the top of the subgrade has been used as the limiting design parameter.

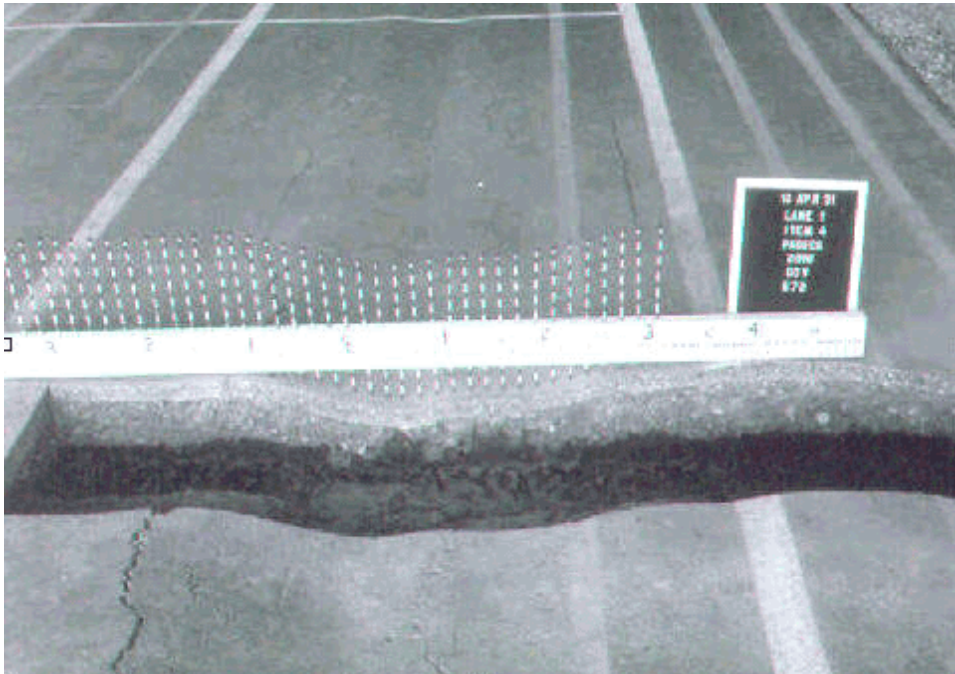


Figure 4 Example of Structural Rutting (17).

Monismith et al. (18) proposed a limiting vertical strain of 200 microstrain. They suggested that computed vertical strains at the top of the subgrade should be kept below this value to

prevent structural rutting. This approach was also recommended by Walubita et al. (19). Instead of limiting the vertical strain, Bejarano and Thompson (20) proposed controlling the vertical stress through the ratio of the vertical stress at the top of subgrade to the unconfined compressive strength of the soil, referred to as the subgrade stress ratio. They recommended using a subgrade stress ratio of 0.42 for design purposes.

2.3 Pavement Thicknesses

For a perpetual pavement design, the limiting tensile strain at the bottom of the asphalt layer and the limiting compressive strain or stress at the top of subgrade can be achieved through choosing appropriate thicknesses and materials for the pavement layers. Minimum and maximum pavement thicknesses have been recommended for a variety of design conditions and summarized in this section. Also discussed in this section are a number of new perpetual pavements designed in recent years.

Based on the analysis of the most heavily traveled pavements in the UK, most of which had carried over 100 million standard axles, Nunn (21) concluded that minimum and maximum thicknesses for long-life full-depth asphalt pavements were 7.9 and 15.4 inches, respectively. This range was determined for a variety of factors. For these pavements, they found little evidence of bottom-up cracking but surface-down cracking that tended to stop at a depth of 4 inches. In addition, for a pavement thicker than 7.1 inches, rutting tended to occur in the asphalt layer.

As part of the Strategic Highway Research Program 2 R23 project, Jackson et al. (22) developed thickness guidelines for long-life (30 to 50 years) asphalt pavement design in the U.S. The development was conducted based on the limiting strain approach for numerous scenarios that simulate field conditions found in five representative locations in the U.S. A minimum thickness of 5.5 inches and a maximum thickness of 14.0 inches were recommended for long-life pavements depending on design conditions including traffic loading and stiffness of foundation support.

There have been several new perpetual pavements built in recent years. The Bradford Bypass in Pennsylvania was designed as a perpetual pavement using both the PerRoad and DAMA programs (23) during the design development phase. Conservative FELs were used for fatigue (70 microstrain) and rutting (200 microstrain). The resulting perpetual pavement consisted of 13.5 inches of AC over 13 inches of aggregate base (23).

In a perpetual pavement experiment in Ontario, four new pavements were constructed. Two were designed according to conventional thickness design (AASHTO '93), and the other two were designed to be perpetual using PerRoad (24). Table 2 summarizes the four designs.

Table 2 Ontario Perpetual Pavement Experiment (24)

Highway	Design Procedure	Traffic, million ESALS (years)	AC Thickness, in.
402	PerRoad	146 (50)	13.4
406	AASHTO '93	42 (50)	9.8
7	AASHTO '93	28 (30)	9.1
Red Hill Creek Expressway	PerRoad	90 (50)	9.4

A perpetual pavement built in Ohio used a threshold of 70 microstrain at the bottom of the AC layer to control cracking (25). The design accounted for the legal load levels plus 20% overload and arrived at 16.25 inches of asphalt over a 6-inch granular base layer.

Historically, perpetual pavement designs in Texas consisted of about 14 inches of AC over approximately 6 inches of lime- or cement-treated base over the subgrade soil. More specifically, it was recommended to have the following (26):

- 1-1.5 inches of permeable friction course (optional)
- 2-3 inches of SMA
- 2-3 inches of coarse graded AC
- ≥8 inches of rut resistant AC
- 2-4 inches of fatigue resistant base AC
- ≥6 inches of lime- or cement-stabilized soil
- subgrade

However, in the same report (26), a slightly modified pavement structure was proposed for use in Texas, as follows:

- 3 inches of SMA
- 3 inches of ¾" Superpave mix
- 8 inches of Type B mix
- 8 inches of lime- or cement-treated soil
- subgrade

Three sections, in two different experiments at the NCAT Pavement Test Track, were found to be perpetual. The first experiment included two sections, N3 and N4, which were built in 2003 with only 9 inches of AC over 6 inches of aggregate base over the track's native subgrade. Though expected to fail after 10 million ESALs, they withstood 30 million and were deemed perpetual (27). The second experiment consisted of two sections built in 2006 for the Oklahoma Department of Transportation. They were constructed on an imported and much poorer subgrade. One section was constructed with 10 inches of AC and was expected to fail, while the other section was constructed with 14 inches of AC as a perpetual pavement (27). The 10 inch section failed and was rehabilitated multiple times while the 14 inch section has exhibited perpetual behavior.

Though every perpetual pavement design is unique and should consider site-specific climate, traffic, soils, and material availability, it appears that a reasonable range of perpetual pavement thickness is between 9 and 16 inches of AC for high volume roadways.

3 EVALUATION AND REFINEMENT OF DESIGN THRESHOLDS

Based on the literature review results, an analysis was conducted as part of this study to evaluate and refine the thresholds for designing perpetual asphalt pavements. The results of this analysis are summarized in this section.

3.1 Fatigue Endurance Limit as Design Threshold

Historically, a perpetual pavement has been designed to have the tensile strain at the bottom of the AC layer below its FEL so that the structure will have infinite fatigue life. In addition, the vertical strain at the top of the subgrade is checked to ensure that it is below a pre-determined

limit to prevent structural rutting. The fatigue endurance limit used in perpetual pavement design is typically determined from laboratory fatigue testing and has ranged in magnitudes from early estimates of 70 microstrain (8) to more recent estimates of up to 200 microstrain (10, 12). A value of 200 microstrain has been proposed for the vertical compressive strain limit (18, 19).

While the perpetual pavement design concept based on FELs has been used successfully to design long life pavements as previously discussed, there is some debate about how high the FEL can be and still maintain a perpetual pavement, and there is also some concern as to whether one limiting strain value can control fatigue cracking.

Since the second research cycle of the NCAT Pavement Test Track started in 2003, fully instrumented pavement sections have been built and evaluated under live truck traffic. Pavement responses collected from these test sections have been used in several studies (16, 28, 29) to evaluate the perpetual pavement design concept based on FEL and to develop a new approach. Tensile strains measured at the bottom of the AC layer in fully instrumented sections in a heavily loaded environment (10 million equivalent single axle loads (ESALs) in each research cycle) were compared with laboratory-determined fatigue endurance limits of the AC base layers. The results of these studies indicated that the number of events in which the strains measured in the field fell below the section’s FEL varied significantly.

Table 3 (28) shows the percent of the field-measured strains that were below the FELs for six test sections from the 2003 and 2006 research cycles of the NCAT Pavement Test Track. For Sections N8, N10, and S11 that experienced fatigue cracking, 3% to 50% of the strains measured in the field fell below the section’s FEL. For Sections N3, N4, and N9 that remained in good condition with no fatigue cracking, 33% to 88% of the field-measured strains fell below the section’s FEL.

Table 3 Comparison of Field Strains and Laboratory FELs (16, 28)

Section, Year	Lab FEL ¹ , microstrain	Percent of Field-Measured Strains Below Section’s FEL ¹	Field Performance
N3, 2003	151	33%	No Fatigue Cracking, Perpetual
N4, 2003	146	38%	No Fatigue Cracking, Perpetual
N8, 2006	203	50%	Fatigue Cracking
N9, 2006	203	88%	No Fatigue Cracking, Perpetual
N10, 2006	130	8%	Fatigue Cracking
S11, 2006	118	3%	Fatigue Cracking

¹FEL was determined as the 95% one-sided lower prediction limit according to the NCHRP 9-38 procedure (10).

Based on the FEL concept, for sections that did not experience fatigue cracking, the percent of field-measured strains below the section’s FEL, as shown in Table 3, should be relatively high, indicating that the majority of the strains fell below the FEL and thus no damage occurred. However, this was not the case. Sections N3 and N4 did not experience fatigue cracking, yet only 33% to 38% of the measured strains fell below the FEL. In this case, the concept of fatigue endurance limit would lead the designer to believe these sections were significantly under-

designed. However, Section N8, a section that failed due to fatigue cracking, showed more promise of being a perpetual pavement with 50% of measured strains less than its FEL. As a result, the researchers were not able to develop correlations between laboratory FELs and pavement performance or field-measured strains. These results suggest that the application of a single fatigue endurance limit may not be an effective design criterion in perpetual pavement design (16, 28).

3.2 Cumulative Strain Distribution as Design Threshold

While the research at the NCAT Pavement Test Track (16) did not find correlations between laboratory FELs and field performance or field-measured strains, they found a noticeable difference between cumulative distributions of field-measured strains for sections that experienced bottom-up fatigue cracking and those that did not, as shown in Figure 5. Each cumulative distribution shown in Figure 5 was determined based on the percent of measured strains less than or equal to a specific strain level. As a result, a field limiting strain distribution (black dashed line in Figure 5) was determined based on field-measured strains for Sections N3 and N4 that did not experience fatigue cracking. It was recommended that the cumulative distribution of tensile strains be further refined for use as limiting criteria for fatigue cracking in the design of perpetual pavements rather than using the FEL (16, 28).

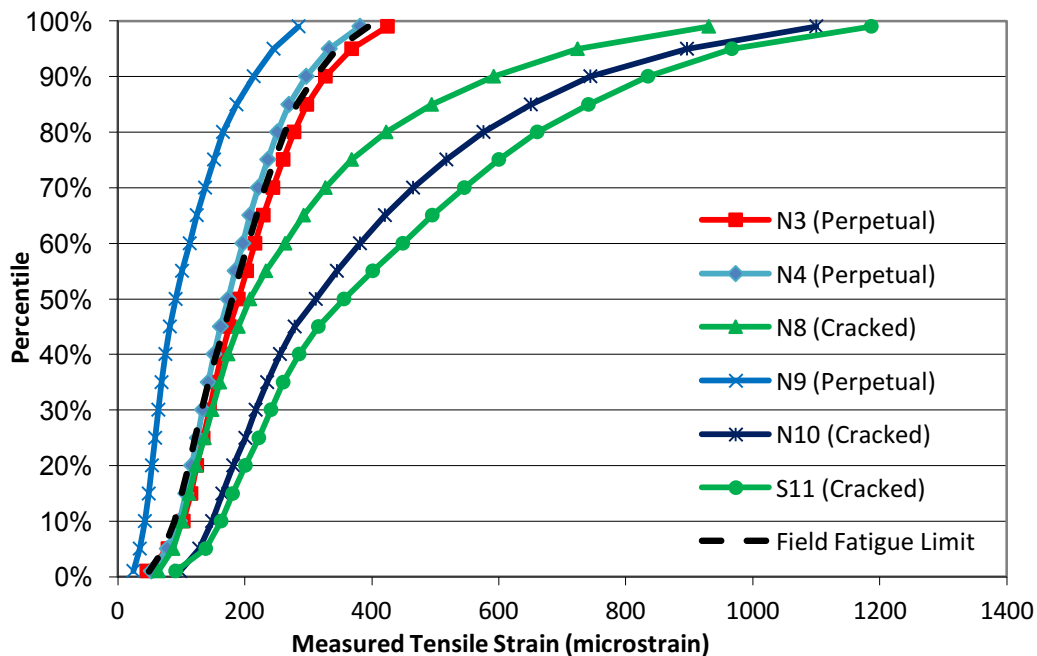


Figure 5 Cumulative Distributions of Measured Strains, Sections Placed in 2003 and 2006 (16, 28).

From the individual cumulative distribution of field strains for each section shown in Figure 5, the researchers determined the fatigue ratios at incremental percentiles, as shown in Figure 6, by dividing the corresponding cumulative strains by the laboratory FEL of the AC base layer. The limiting fatigue ratios (black dashed line in Figure 6) were a result of the distinct difference

between sections that experienced fatigue cracking and those that did not. These studies showed that the fatigue ratios of the pavement sections that did not experience fatigue cracking fell below the limiting fatigue ratios (16, 28).

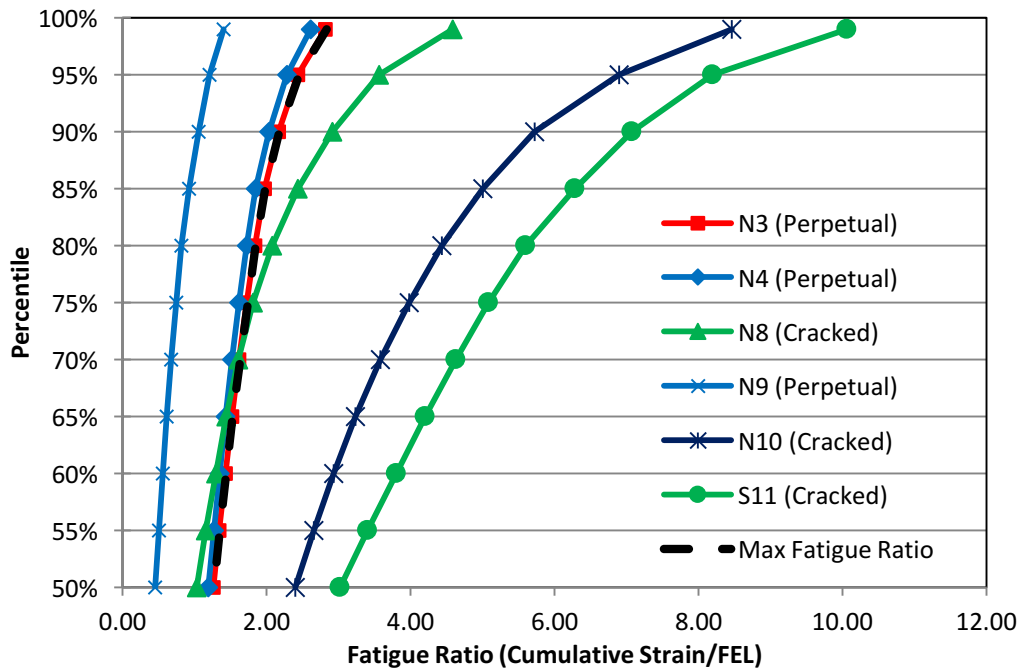


Figure 6 Fatigue Ratios based on Strains Measured in 2006 Cycle and FEL after (16, 28).

The limiting strain distribution (Figure 5) and maximum fatigue ratios (Figure 6) show promise for perpetual pavement design; however, they were determined based on field-measured strains. Past studies at the NCAT Pavement Test Track have shown differences between field-measured strains and predicted tensile strains at the bottom of the AC layer (30, 31). Figures 7 and 8 compare the cumulative distributions of field-measured strains with strains predicted by PerRoad for the cracked and perpetual sections, respectively. These figures show that cumulative distributions from measured strain values are much higher than the corresponding cumulative distributions of tensile strain values predicted by PerRoad. These differences could in part be attributed to the differences in the definition of strain in the field and what is used in PerRoad. Field-measured strain was based on the amplitude of the strain trace such that strain was defined as the magnitude from the trough to peak strain, whereas PerRoad considers only the peak strain, or the difference between the baseline and the peak in the strain trace. Previous research at the test track has shown that strain measured by the amplitude can be 20% to 30% higher than strain defined by the peak value (32). In this case, the measured strains are approximately 80% higher than the predicted strains at the 50th percentile for Sections N3 and N4.

Thus, the limiting strain distribution and maximum fatigue ratios developed based on field-measured strains may not be readily applicable to predicted strains resulting from perpetual pavement design. Therefore, there is a need to refine the limiting strain distribution and fatigue

ratios shown in Figures 5 and 6 to reflect predicted strains determined in perpetual pavement design and to validate the refined criteria for future implementation.

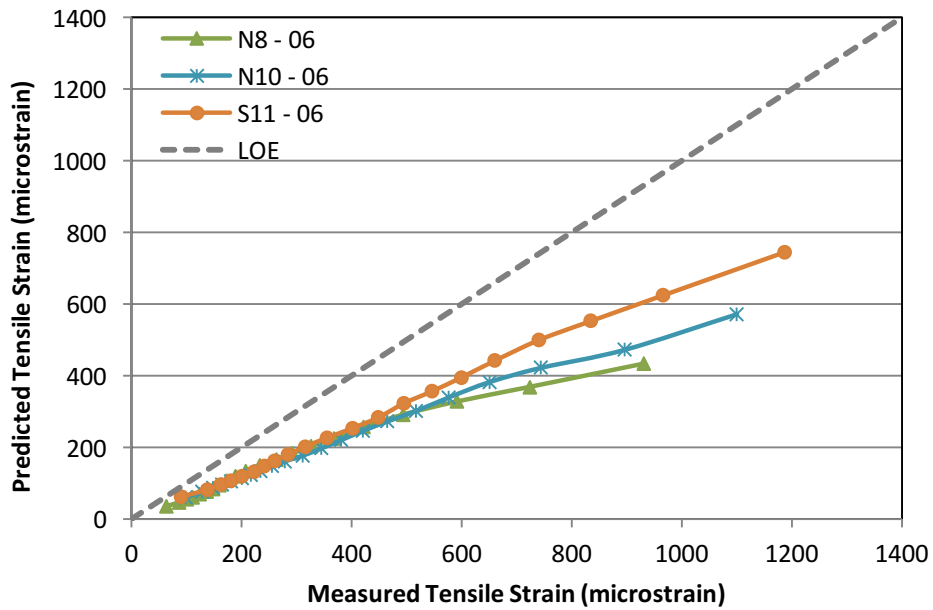


Figure 7 Measured versus Predicted Cumulative Strain Distributions for (Fatigue) Cracked Sections (29).

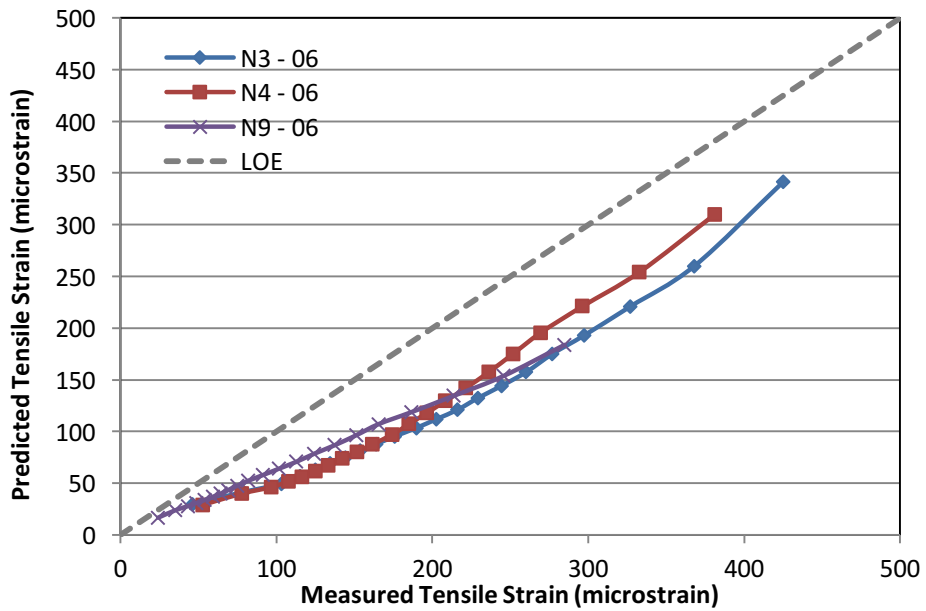


Figure 8 Measured versus Predicted Cumulative Strain Distributions for Perpetual Sections (29).

3.3 Refining Design Thresholds for Perpetual Pavement Design

The focus of the second part of this study was two-fold:

1. to refine the limiting strain distribution and maximum fatigue ratios developed by Willis and Timm (16) to reflect the differences between measured and predicted strain values for future implementation in perpetual pavement design, and
2. to validate the refined limiting strain distribution and maximum fatigue ratios.

For this analysis, two sections built in the 2003 research cycle of the NCAT Pavement Test Track and four sections built in the 2006 research cycle were simulated in PerRoad version 3.5 to predict tensile strain values at the bottom of the AC layer. These sections were used to refine the limiting strain distribution based on predicted strain values for use in perpetual pavement design. Additionally, six sections from the 2009 research cycle were used to validate the refined limiting strain distribution. The results of this analysis (as presented below) were adapted from a previous report (29).

3.3.1 Pavement Sections and Field Performance

Twelve sections from three research cycles at the NCAT Pavement Test Track were selected for this analysis. The selected sections were placed on the north and south tangents of the 1.7-mile oval track, a full-scale accelerated loading facility, located in Opelika, Alabama. Each research cycle of the NCAT Pavement Test Track operates on a three-year period, with two years designated for trafficking and one year split between construction and forensic evaluation at the conclusion of the traffic period. Approximately 10 million ESALs are applied over a two-year traffic period with a fleet of five triple trailer trucks operating at 45 mph for 16 hours a day, five days a week. The triple trailer trucks consist of a 12-kip steer axle, a 40-kip tandem axle, and five trailing 20-kip single axles. Weekly performance evaluations including crack mapping, rut-depth measurement, and ride-quality measurements are augmented by frequent falling-weight deflectometer testing and strain-response measurements.

Figure 9 shows cross sections and Table 4 lists quality control (QC) asphalt mixture properties for 12 pavement sections built in three research cycles at the track selected for this study. Two pavement sections, including N3 and N4, were built in 2003, and four sections, including N8, N9, N10, and S11, were built in 2006. The remaining six sections, N10, N11, S8, S9, S10, and S11, were from the 2009 research cycle. A brief description of each test section selected for this analysis follows.

Sections N3 and N4 were placed as part of the 2003 research cycle and were left in place through the end of the 2009 research cycle. These sections were designed with nine inches of AC over six inches of granite base material and the test track subgrade material, classified as an AASHTO A-4(0) soil. These two sections were designed to replicate each other with the exception of the binder type. Section N3 used a performance grade (PG) 67-22 unmodified binder throughout the AC layer, and section N4 used a PG 76-22 modified with styrene-butadiene-styrene (SBS) throughout.

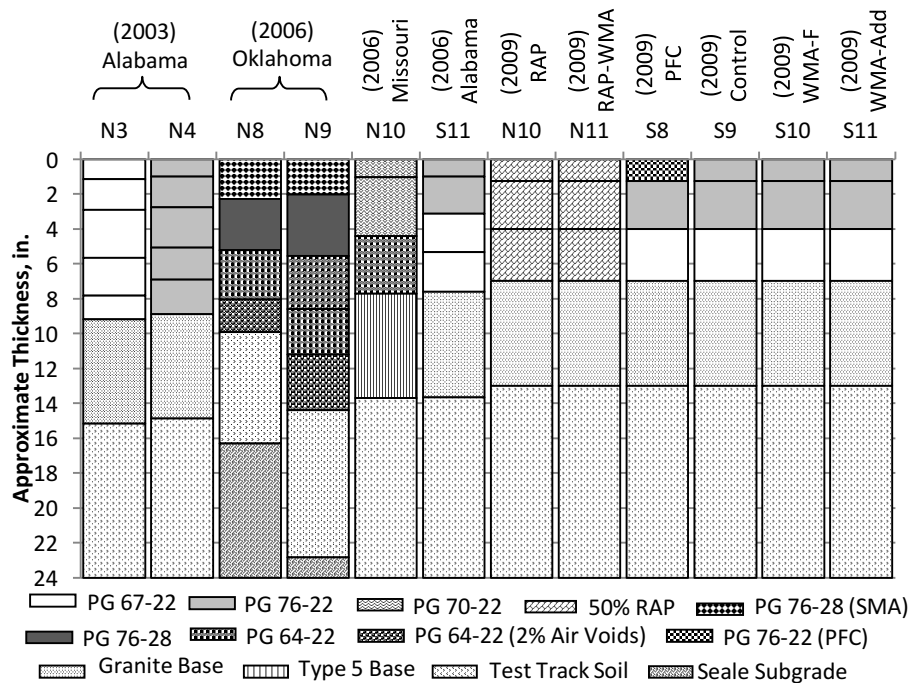


Figure 9 Cross Sections and Materials of Test Sections Used in This Analysis.

In the 2006 research cycle, Section N8 was designed with 10 inches of AC including a stone-mastic asphalt (SMA) surface lift, conventional AC layers using PG 76-28 and PG 64-22 binders, and a rich-bottom layer designed at 2% air voids with PG 64-22 binder. Section N9 was the complement to N8, although it was designed to be perpetual at 14 inches of AC. Sections N8 and N9 used the same mixtures throughout. Both sections N8 and N9 used the compacted test track soil as a base material and a compacted soft subgrade material over the existing track soil subgrade. Section N9 was left in place through the 2009 track cycle and as part of the 2012 test cycle. Section N10 was designed at eight inches of AC consisting of mixes with PG 70-22 binder in the surface and intermediate layer and PG 64-22 binder in the base course mix. Six inches of a type-5 base material from Missouri was used as a granular base layer over the test track subgrade. Lastly, Section S11 was designed at seven inches of AC, featuring a PG 76-22 SBS-modified binder in the top two AC lifts and PG 64-22 in the bottom two lifts, on top of six inches of granite base material and the track soil subgrade. Detailed information about these sections can be found in a previous report (33).

Test sections placed as part of the 2009 research cycle used for this study included six of the eight-section group experiment: N10, N11, S8, S9, S10, and S11. These sections were all designed at 7 inches of AC on top of 6 inches of granite base, placed on top of the test track subgrade material. These sections were selected due to the range in mix types used and although many were unconventional, they used commonly available technology. Additionally, all of these sections experienced bottom-up fatigue cracking and would serve well for validating the refined limiting distribution of predicted strains.

Table 4 QC Properties of Asphalt Mixtures

Cycle	Section	Layer	NMAS	Aggregate	PG	Polymer	%RAP	WMA	%Pb	%Va	%VMA	%Vbe
2003	N3	1	9.5	Grn/Lms/Snd	67-22	No	0	No	6.1	5.7	17.0	11.3
		2	19	Lms/Grn/Snd	67-22	No	0	No	4.3	4.7	14.0	9.3
		3	19	Lms/Grn/Snd	67-22	No	0	No	4.5	3.1	13.0	9.9
		4	19	Lms/Grn/Snd	67-22	No	0	No	4.3	5.1	16.0	10.9
		5	19	Lms/Grn/Snd	67-22	No	0	No	4.6	4.0	15.0	11.0
	N4	1	9.5	Grn/Lms/Snd	76-22	SBS	0	No	6.1	5.5	19.0	13.5
		2	19	Lms/Grn/Snd	76-22	SBS	0	No	4.3	4.7	15.0	10.3
		3	19	Lms/Grn/Snd	76-22	SBS	0	No	4.4	3.3	14.0	10.7
		4	19	Lms/Grn/Snd	76-22	SBS	0	No	4.7	3.0	14.0	11.0
		5	19	Lms/Grn/Snd	76-22	SBS	0	No	4.4	4.5	15.0	10.5
2006	N8	1	12.5	Granite	76-28	SBS	0	No	6.9	5.0	15.6	10.6
		2	19	Granite	76-28	SBS	0	No	5.2	2.8	10.4	7.6
		3	19	Granite	64-22	No	0	No	4.9	4.4	11.3	6.9
		4	12.5	Granite	64-22	No	0	No	7.1	2.1	12.6	10.5
	N9	1	12.5	Granite	76-28	SBS	0	No	7.0	4.9	15.5	10.6
		2	19	Granite	76-28	SBS	0	No	5.1	3.0	10.5	7.5
		3	19	Granite	64-22	No	0	No	5.0	3.4	10.4	7.0
		4	19	Granite	64-22	No	0	No	4.6	3.8	10.4	6.6
		5	12.5	Granite	64-22	No	0	No	7.0	1.7	12.2	10.5
	N10	1	12.5	Porphyry	70-22	SBS	0	No	5.6	5.6	16.9	11.3
		2	19	Porphyry	70-22	SBS	0	No	4.7	4.4	13.7	9.3
		3	19	Porphyry	64-22	No	0	No	5.2	4.1	14.2	10.1
	S11	1	9.5	Grn/Lms/Snd	76-22	SBS	0	No	6.9	3.4	18.0	14.6
		2	19	Lms/Grn/Snd	76-22	SBS	0	No	5.4	4.6	15.6	11.0
		3	19	Lms/Grn/Snd	67-22	No	0	No	5.0	4.9	15.1	10.2
		4	19	Lms/Grn/Snd	67-22	No	0	No	4.9	5.2	15.3	10.1
2009	N10	1	9.5	RAP/Snd/Grn	67-22	No	50%	No	6.0	3.8	15.8	12.0
		2	19	RAP/Lms/Snd	67-22	No	50%	No	4.4	4.5	13.6	9.1
		3	19	RAP/Lms/Snd	67-22	No	50%	No	4.7	4.2	13.8	9.6
	N11	1	9.5	RAP/Snd/Grn	67-22	No	50%	Foam	6.1	3.2	15.5	12.3
		2	19	RAP/Lms/Snd	67-22	No	50%	Foam	4.7	3.7	13.6	9.9
		3	19	RAP/Lms/Snd	67-22	No	50%	Foam	4.6	4.1	13.7	9.6
	S8	1	12.5	Grn/RAP	76-22	SBS	15%	No	5.1	NA	NA	NA
		2	19	Lms/Snd/Grn	76-22	SBS	0	No	4.6	4.1	13.8	9.7
		3	19	Lms/Snd/Grn	67-22	No	0	No	4.9	3.6	14.0	10.4
	S9	1	9.5	Grn/Snd/Lms	76-22	SBS	0	No	6.1	4.0	16.5	12.5
		2	19	Lms/Snd/Grn	76-22	SBS	0	No	4.4	4.4	13.5	9.1
		3	19	Lms/Snd/Grn	67-22	No	0	No	4.7	4.0	13.9	9.9
	S10	1	9.5	Grn/Snd/Lms	76-22	SBS	0	Foam	6.1	3.3	16.0	12.7
		2	19	Lms/Snd/Grn	76-22	SBS	0	Foam	4.7	4.6	14.3	9.7
		3	19	Lms/Snd/Grn	67-22	No	0	Foam	4.7	4.1	14.0	9.9
	S11	1	9.5	Grn/Snd/Lms	76-22	SBS	0	Adtv	6.4	3.4	16.7	13.3
		2	19	Lms/Snd/Grn	76-22	SBS	0	Adtv	4.6	4.9	14.5	9.6
		3	19	Lms/Snd/Grn	67-22	No	0	Adtv	5.0	3.0	13.7	10.7

In the 2009 research cycle, S9 served as the control section for the group experiment and featured conventional AC mixtures including a surface course utilizing PG 76-22 SBS-modified binder, an intermediate layer also using a PG 76-22 SBS-modified binder, and a base course using conventional PG 67-22 binder. Section S8 mirrored section S9 with the exception of the surface layer, which replaced the conventional mix with a porous friction course (PFC) designed with 15% reclaimed asphalt pavement (RAP) at the same thickness of 1.25 inches. Sections N10 and N11 shared the same mix designs including 50% RAP in all three AC layers. The difference between these sections was that N11 used foaming technology to produce it as a warm-mix asphalt (WMA) while N10 was produced at typical production temperatures for hot-mix asphalt (HMA). Sections S10 and S11 shared mix designs with Section S9 but were produced using warm-mix technologies. Section S10 was produced with foaming technologies and Section S11 incorporated an additive to achieve production at warm-mix temperatures.

3.3.2 Field Performance

Sections N3, N4, and N9 exhibited no signs of bottom-up fatigue cracking. Sections from the 2006 research cycle that experienced bottom-up fatigue cracking were Sections N8, N10, and S11. Sections N3 and N4 (built in 2003) remained in service during both the 2006 and 2009 research cycles. These sections were in excellent condition with only minor longitudinal cracking after approximately 30 million ESALs. Forensic investigations at the conclusion of the 2009 cycle revealed that longitudinal cracking in both sections was top-down and that no bottom-up fatigue cracking was evident in section N4. Section N3 experienced a subsurface crack likely due to the adjacent embedded instrumentation and therefore was still considered perpetual in nature (34). Section N9 was built in 2006 and left in place through the 2009 research cycle. During this second cycle, the section experienced longitudinal cracking near the centerline after cumulative traffic loads in excess of 16 million ESALs. Top-down cracking at the Pavement Test Track has historically appeared as longitudinal cracking. Cores were cut at the location of the longitudinal crack, from which it was confirmed that the cracking was top-down. Section N9 was left in place for continuing traffic as part of the 2012 research cycle, and after approximately 28 million ESALs, it only exhibits evidence of top-down cracking.

Six sections (N10, N11, and S8 through S11) placed as part of the 2009 NCAT Pavement Test Track performed well during the two-year trafficking period with little to no distresses evident and no fatigue cracking at the conclusion of the research cycle and application of 10 million ESALs. The six sections were left in place for the 2012 research cycle, during which time distresses became visible. Cracking was observed in all six sections.

Cores were extracted in four sections of the six sections (S8 through S11). The cores confirmed that for Sections S8 through S11, the transverse cracking was bottom-up and the longitudinal cracking was top-down. Transverse cracking in S8 was first observed in the spring of 2013 after just over 12 million cumulative ESALs, and longitudinal cracking was later evident as well. In a similar fashion, Section S9 also exhibited longitudinal and transverse cracking during the 2012 research cycle. Cracking was first observed in March of 2013 in the longitudinal direction after approximately 12 million cumulative ESALs and transverse cracking was observed shortly thereafter. Section S10 experienced both transverse and longitudinal cracking, which was first observed in January of 2013. Longitudinal cracking was first observed in Section

S11 in December of 2012 after 10.7 million cumulative ESALs and transverse cracking was evident by the following spring (2013).

Section N10 was the last of the six sections continued from 2009 to crack. Transverse cracking was observed in Section N10 in November of 2013 after a combined 15.5 million ESALs had been applied. However, this initial transverse cracking was in an area immediately adjacent to a patch placed to correct an area of severe but localized distress. Transverse cracking was observed in other areas in the section by February of 2014. Cores were not extracted in this section; however, it is believed that the transverse cracking originated at the bottom of the AC layer and propagated to the surface, as was the case in Sections S8 through S11. Section N11 also experienced transverse cracking, and although cores were not extracted it likely propagated from the bottom of the AC to the surface. Longitudinal cracking was first observed in Section N11 in February of 2013 and transverse cracking was evident shortly thereafter. There was extensive cracking that became interconnected in the outside wheel path. This area of interconnected cracking was the site of the initial observations of transverse cracking. Table 5 summarizes the performance of the 2003, 2006, and 2009 test sections included in this analysis; shading indicates sections that did not experience fatigue cracking.

Table 5 Field Performance of Test Sections Used in this Perpetual Pavement Analysis

Section	AC Thickness (in.)	Year Built	Fatigue Cracking
N3	9.17	2003	No
N4	8.89	2003	No
N8	9.92	2006	Yes
N9	14.40	2006	No
N10	7.71	2006	Yes
S11	7.61	2006	Yes
N10	7.09	2009	Yes
N11	7.12	2009	Yes
S8	7.04	2009	Yes
S9	7.00	2009	Yes
S10	7.00	2009	Yes
S11	6.90	2009	Yes

3.3.3 Analysis Methodology

In this analysis, the stochastic perpetual pavement design software, PerRoad version 3.5, was utilized to predict horizontal tensile strain at the bottom of the AC layer for the twelve pavement sections. The software utilizes Monte Carlo simulation to allow for the consideration of known variability associated with material properties and construction as well as seasonal variation effects on material moduli. Using the software, pavement responses at critical locations were determined from which strain distributions based on PerRoad predictions were computed and fatigue ratios were then developed.

For each section, PerRoad was utilized to complete Monte Carlo simulations, generating 5,000 predictions of tensile strain at the bottom of the AC layer. Cumulative distributions were developed from the predicted strain for each section to compare with the previously developed

cumulative distributions from field-measured strains. To predict tensile strain at the bottom of the AC layer using PerRoad, load spectra, pavement layer moduli, thickness, and the associated coefficient of variation (COV) for each were necessary. A description of each input follows.

Load Spectra. Axle weights for each of the five triple trailer trucks used to apply traffic at the NCAT Pavement Test Track were determined previously (35). Based on the total number of axles in the fleet, it was determined that single axles represented 71.42% of the total number of axles applied and the steer and tandem axles each accounted for 14.29% of applied axles. The axle weights for each axle type (steer, tandem, and single) were entered into PerRoad to characterize the traffic loadings in the form of load spectra: 20% of the steer axles weighed 8-10 kips, with the remaining 80% falling into the 10-12 kip range; 80% of the tandem axles weighed between 38 and 40 kips, with the remaining percentage weighing between 40 and 42 kips; and 100% of the single axles weighed between 20 and 22 kips.

Cross-Sections. A three-layer structure was selected for each section with layer one representing the AC, and layers two and three representing the unbound granular base and subgrade, respectively. Four random locations were identified at the start of each test cycle and it was at these four locations in the outside, between, and inside wheelpaths that layer thickness was surveyed during construction. From these measurements, the average layer thicknesses were determined for each section as well as the coefficient of variation (COV) of the layer thickness, as listed in Table 6. Sections N3 and N4 were originally constructed in 2003 and did not have surveyed thicknesses of the unbound granular base layer. Therefore, the sections were assumed to have a thickness equivalent to their design layer thickness of 6 inches and a COV equivalent to the average COV for the unbound granular base (GB) layer in the 2009 sections. A normal distribution was assigned to the layer thickness variability.

Material Inputs. Falling weight deflectometer (FWD) testing was also conducted at four random locations in the outside, between, and inside wheelpaths throughout the duration of each test cycle. FWD testing included three replicates at four drop heights (load levels). Measured deflections were used to conduct a three-layer (AC, unbound base, and subgrade layers) backcalculation in EVERCALC version 5.0. Section-specific unbound base and subgrade layer inputs were determined by calculating the average layer modulus for the entire two-year trafficking period. Average backcalculated layer moduli were selected for the 9-kip load level (load corrections were not applied) with root mean square error (RMSE) less than 3%. The backcalculated base and subgrade moduli at the 9-kip load level are listed in Table 7 along with their associated COV. For the PerRoad simulations, a normal distribution was used in conjunction with the COVs listed in Table 7 for the backcalculated layer moduli of both the unbound base layer and subgrade material in each section. Although constructed in 2003, N3 and N4 remained in-service for 2006 and 2009 test cycles. For the analysis conducted in this study, backcalculated moduli from the 2006 test cycle were utilized for the analysis of sections N3 and N4; as such, these sections are labeled with the year 2006 in reference to predicted strains.

Table 6 Layer Thickness and Associated Variability By Section

Section	h_{AC} (in.)	COV_{AC} (%)	h_{GB} (in.)	COV_{GB} (%)
N3 (2006) ¹	9.17	2.4	6	8.8
N4 (2006) ¹	8.89	3.8	6	8.8
N8 (2006)	9.92	6.2	6.38	5.1
N9 (2006)	14.40	4.0	8.44	9.7
N10 (2006)	7.71	3.2	6.00	8.4
S11 (2006)	7.61	7.5	6.08	14.2
N10 (2009)	7.09	3.3	3.98	12.6
N11 (2009)	7.12	2.6	4.22	7.9
S8 (2009)	7.04	3.0	5.51	7.2
S9 (2009)	7.00	2.3	5.80	4.9
S10 (2009)	7.00	3.6	6.35	6.4
S11 (2009)	6.90	2.3	6.17	7.1

¹Originally constructed in 2003

Table 7 Unbound Layer Moduli and Associated Variability

Section	Base (ksi)	Subgrade (ksi)	COV_{GB} (%)	COV_{SG} (%)
N3 (2006)	6.34	34.25	59.5	14.5
N4 (2006)	4.63	32.90	57.7	16.0
N8 (2006)	3.70	32.29	32.6	13.7
N9 (2006)	3.24	56.56	39.1	25.9
N10 (2006)	2.80	46.93	39.2	11.8
S11 (2006)	2.46	31.12	35.6	10.9
N10 (2009)	2.11	44.75	43.4	12.1
N11 (2009)	3.27	38.52	38.5	8.4
S8 (2009)	2.85	23.25	58.4	11.9
S9 (2009)	2.08	26.16	39.5	15.1
S10 (2009)	1.64	26.19	36.0	14.3
S11 (2009)	1.66	26.32	31.7	17.2

PerRoad allows for AC moduli to be entered for up to five seasons. First, section-specific modulus-temperature relationships of the form listed in Equation 1 were developed with backcalculated AC moduli and the mid-depth pavement temperatures recorded throughout the two-year testing cycles. The backcalculated moduli selected for the modulus-temperature relationship were at the 9-kip load level and RMSE less than 3%. Hourly average temperatures were recorded for each section during the entire two-year trafficking period. The average hourly mid-depth pavement temperatures were then used in the modulus-temperature relationship to develop a cumulative distribution of AC moduli experienced throughout the trafficking period. Once developed, the cumulative distribution of the AC moduli was used to select seasonal moduli in each section. The midpoint of each quintile was selected as the representative AC modulus for each of the five seasons: summer (10th percentile), spring 2

(30th percentile), spring (50th percentile), fall (70th percentile), and winter (90th percentile). These moduli are listed in Table 8 for each test section. PerRoad requires the user to input the number of weeks in each season; therefore, 10 weeks were assigned to spring, fall, and winter, while summer and spring 2 were each assigned 11 weeks to be conservative. The COV for the AC modulus was calculated from temperature-corrected AC moduli. To do so, the backcalculated AC moduli, E_1 , were corrected to 68°F, using Equation 2, and then the average and standard deviation of the corrected moduli were calculated to determine the COV. The COV for the corrected AC moduli are also listed in Table 8 for each test section. A log-normal distribution of AC moduli for each section was selected for the PerRoad simulations.

$$E_1 = \alpha_1(e^{\alpha_2 T}) \tag{1}$$

where

- E_1 = AC modulus (psi);
- α_1, α_2 = regression coefficients; and
- T = mid-depth pavement temperature (°F).

$$E_{T_r} = E_1(e^{\alpha_2(T_r - T)}) \tag{2}$$

where

- E_1 = AC modulus at T (psi);
- E_{T_r} = AC modulus at T_r (psi);
- T = mid-depth pavement temperature (°F); and
- T_r = reference temperatures, 68°F.

Table 8 AC Variability and AC Moduli by Season for PerRoad Simulations

Section	COV (%)	Design Modulus, ksi				
		Summer	Spring 2	Spring	Fall	Winter
N3 (2006)	36.5	302.29	517.86	733.32	1022.28	1536.61
N4 (2006)	22.5	306.32	516.40	852.54	1309.14	1925.96
N8 (2006)	19.3	155.01	287.76	476.78	833.04	1333.62
N9 (2006)	22.4	240.45	384.75	654.68	977.31	1361.62
N10 (2006)	17.6	178.10	315.85	539.74	821.80	1197.28
S11 (2006)	17.2	139.64	249.47	451.50	760.88	1159.49
N10 (2009)	12.0	351.80	575.77	882.59	1432.38	2240.17
N11 (2009)	8.8	312.14	499.75	771.00	1288.27	2009.92
S8 (2009)	16.6	254.10	394.25	579.65	911.68	1386.25
S9 (2009)	12.5	249.20	397.99	632.82	1109.39	1794.56
S10 (2009)	11.5	232.54	390.86	597.95	996.86	1599.14
S11 (2009)	14.6	234.02	379.66	610.51	1018.44	1616.85

Fatigue Ratios. The maximum fatigue ratios based on the predicted strains were determined using Equation 3.

$$R_n = \epsilon_n / \epsilon_f \tag{3}$$

where

- R_n = fatigue ratio at the n^{th} percentile;
- ϵ_n = microstrain at the n^{th} percentile; and
- ϵ_f = laboratory-determined fatigue threshold or endurance limit, microstrain.

The laboratory-determined fatigue endurance limits for the 2003 sections (N3 and N4) were established by first conducting BBFT on samples compacted to 7.0% target air voids in accordance with AASHTO T321. As documented by Willis and Timm (16), the fatigue endurance limit was determined as part of the NCHRP 9-38 project (10) by applying a three-stage Weibull equation and was taken as the 95% one-sided lower prediction limit. The fatigue endurance limits for the 2006 sections were also determined in the same manner; however, samples were compacted to 5.5% target air voids at two strain levels, 400 and 800 microstrain (28). Bending beam fatigue testing was also conducted for the base AC mixtures in the 2009 sections following AASHTO T321 using specimens compacted to target air voids of 7.0% and tested at strain levels of 200, 400, and 800 microstrain. Lower target air voids were selected for BBFT of the sections placed in 2006 to be representative of the rich bottom layer (low air voids mix) utilized in sections N8 and N9. The remaining sections placed in 2006 were also evaluated at the same air void level to enable relative comparisons among the sections. Table 9 provides the fatigue endurance limits taken as the 95% one-sided lower prediction for the selected sections.

Table 9 Laboratory Fatigue Endurance Limit after (16, 28)

Section	Endurance Limit - 95 th one-sided lower prediction limit, microstrain	Target Air Voids of BBFT Specimens
N3 (2003)	151	7.0%
N4 (2003)	146	7.0%
N8 (2006)	203	5.5%
N9 (2006)	203	5.5%
N10 (2006)	130	5.5%
S11 (2006)	118	5.5%
N10 (2009)	100	7.0%
N11 (2009)	134	7.0%
S8 (2009)	92	7.0%
S9 (2009)	92	7.0%
S10 (2009)	99	7.0%
S11 (2009)	84	7.0%

3.3.4 Refined Limiting Strain Criteria for Use in Perpetual Pavement Design

As a result of the PerRoad simulations, tensile strains were predicted at the bottom of the AC layer in each test section under the applied load spectra accounting for seasonal variation in AC moduli and measured variability in layer moduli and thickness. Using the predicted tensile strains, a cumulative strain distribution was determined for each section. Figure 10 compares the predicted cumulative strain distributions for the 2006 test sections.

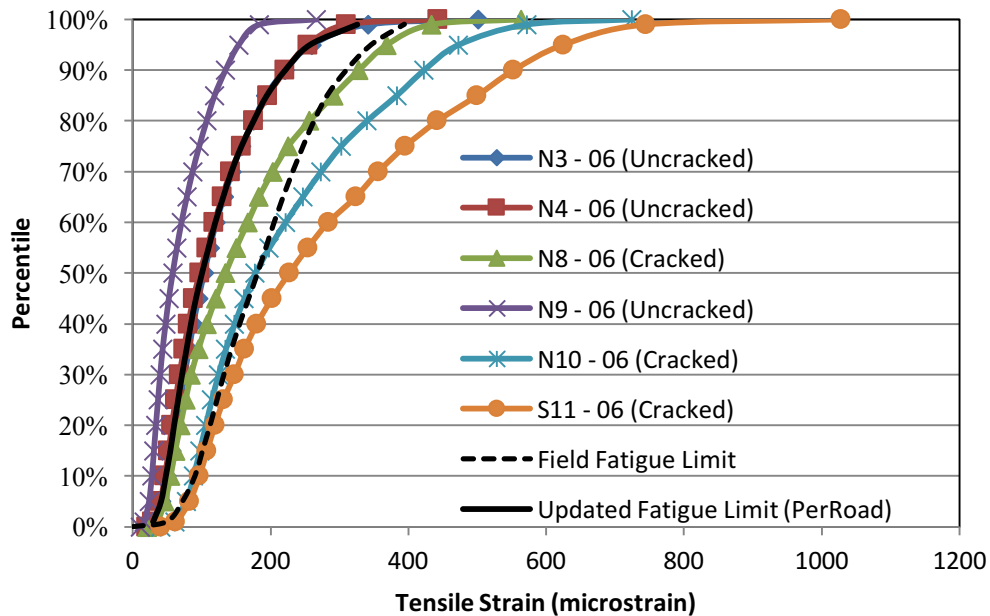


Figure 10 Cumulative Distributions of Predicted Tensile Strain, 2006 Sections.

As shown in Figure 10, there is an obvious separation at the predicted cumulative strain distributions for Sections N3 and N4, as all sections where predicted strain distributions fall to the right of these curves exhibited bottom-up fatigue cracking and all sections where predicted strain distributions fall to the left did not. This is consistent with the observations made from field-measured strains in the previous study (16). Since the cumulative distributions for predicted strains in Sections N3 and N4 lie nearly on top of one another and because these sections have the highest strain levels without experiencing fatigue cracking, they were selected for refining the limiting cumulative distribution of predicted tensile strains. To do so, consistent with the same methodology followed for developing the field-based limiting strain distribution, the average of the N3 and N4 predicted strain values at each percentile level were determined and plotted as a black solid line with the cumulative distributions of predicted strains of the other sections in Figure 10. For comparison, the field-based distribution is also shown in Figure 10 as a black dashed line. Values for this new limiting distribution based on predicted strains are listed in Table 10.

Table 10 Refined Limiting Distribution and Maximum Fatigue Ratios for Predicted Tensile Strain

Percentile	Limiting Design Distribution for Predicted Strain	Maximum Fatigue Ratio for Predicted Strain
1%	29	
5%	41	
10%	48	
15%	54	
20%	60	
25%	66	
30%	71	
35%	78	
40%	84	
45%	91	
50%	100	0.68
55%	110	0.74
60%	120	0.81
65%	131	0.88
70%	143	0.96
75%	158	1.06
80%	175	1.18
85%	194	1.31
90%	221	1.49
95%	257	1.73
99%	326	2.19

The predicted strain values of N3 and N4 at each percentile level were divided by the corresponding FELs (Table 9) to determine the fatigue ratios for these sections. The average ratio of N3 and N4 for each percentile was then calculated to refine the maximum fatigue ratios to reflect tensile strain values predicted in PerRoad. The refined maximum fatigue ratios are listed in Table 10. Figure 11 compares the refined maximum fatigue ratios (black solid line) to those of the other 2006 sections evaluated. Ratios that fail the criteria are on the right of the max fatigue ratio line (labeled “Updated Fatigue Ratio (PerRoad)”). As expected, Sections N10 and S11 fail these criteria. However, Section N8, a section that experienced fatigue cracking, barely passes the criterion at the 50th, 55th, and 99th percentile. For these criteria to serve as an indicator of the ability of a perpetual pavement design to withstand bottom-up fatigue cracking, the criteria at all percentiles from the 50th through the 99th percentile should be met. Despite a predicted strain distribution that is clearly far to the right of the refined cumulative distribution, N8 had fatigue ratios that barely failed. This can be attributed to its very high laboratory-determined fatigue endurance limit of 203 microstrain.

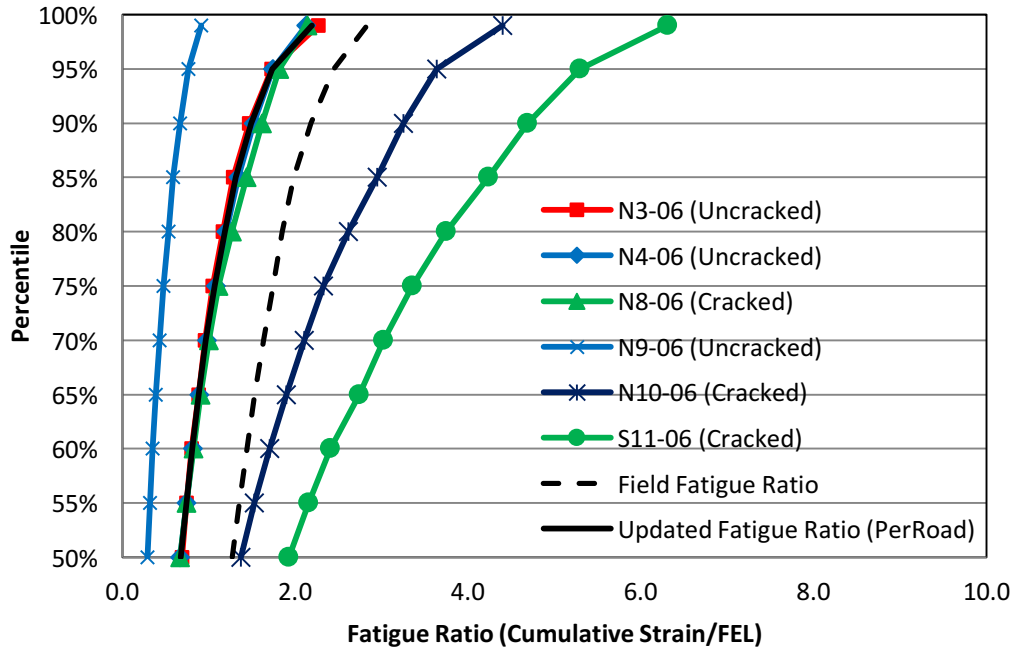


Figure 11 Fatigue Ratios based on Predicted Strains and FEL, 2006 Sections.

3.3.5 Validating Refined Design Thresholds

To determine if the refined limiting strain criteria (cumulative distribution and maximum fatigue ratios based on predicted strains) were valid, six sections from the 2009 research cycle were simulated in PerRoad. The resulting predicted tensile strain values were used to develop cumulative strain distributions as was done with the 2006 test sections. Figure 12 shows the predicted strain distributions for each of the 2009 sections with the refined limiting cumulative distribution as well as the original field-based limiting strain distribution for comparison. All six sections from 2009 are believed to have bottom-up fatigue cracking (four of the sections have been confirmed with field cores and the other two exhibit cracking consistent with bottom-up cracking historically observed at the test track). As was the case with predicted strain distributions for the 2006 sections, the field-based limiting strain distribution did not effectively categorize sections prone to fatigue cracking based on predicted strain values. Predicted strain distributions for sections N10 and N11 both fall to the left of the field-based limiting strain distribution, which would indicate that they passed this criteria. This is again an artifact of the underprediction of tensile strains. Since field-measured strains are not available during the design process, the limiting strain distribution based on predicted strains from PerRoad is necessary for perpetual pavement design. The design limiting strain distribution, shown in Figure 12 as “Updated Fatigue Limit”, accurately categorizes all six sections as prone to fatigue cracking. All six predicted strain distributions fall to the right of the design limiting distribution and all six sections experienced bottom-up fatigue cracking. This evaluation validates the refined limiting strain distribution based on predicted strain values for use in perpetual pavement design.

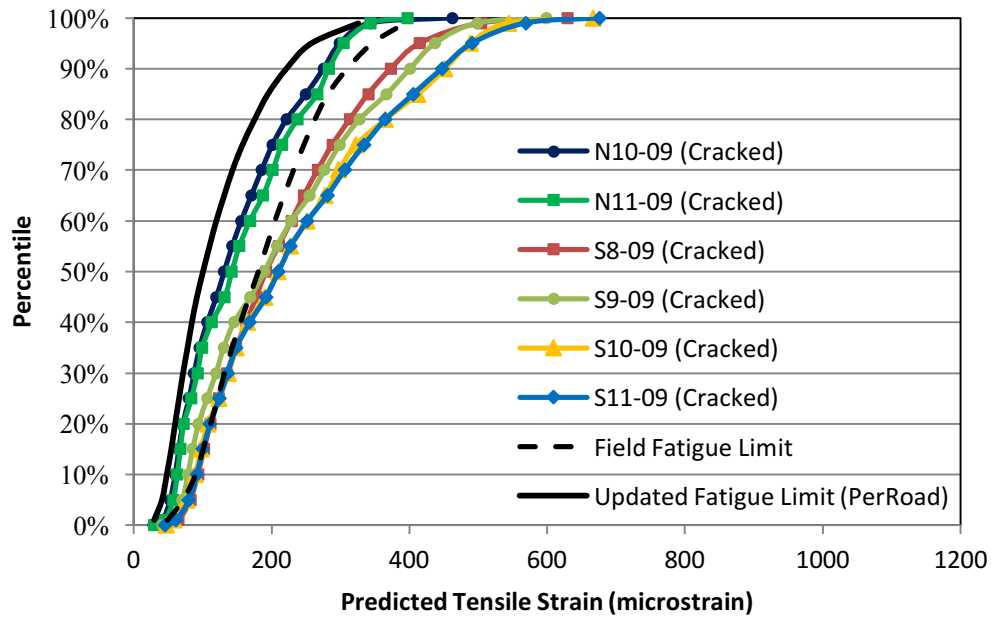


Figure 12 Validating Refined Limiting Fatigue Distribution Using 2009 Sections.

Fatigue ratios were determined for the 2009 test sections using the predicted strain distributions shown in Figure 12 and the associated fatigue endurance limits listed in Table 9. The 2009 test sections served as a validation data set, as they were not used to refine the field-based strain distribution and maximum fatigue ratios to incorporate predicted strain values. Figure 13 shows the fatigue ratios for each of the 2009 test sections, the refined maximum fatigue ratios, and the field fatigue ratios. The maximum fatigue ratios were refined to reflect predicted strains for use in design. The maximum fatigue ratios are meant to serve as criteria for perpetual pavement design such that ratios at all percentiles from 50 to 99 should be less than the maximum fatigue ratios to achieve a section that will behave perpetually, as did sections N3, N4, and N9. It is expected that since all six sections from the 2009 research cycle experienced bottom-up fatigue cracking, the fatigue ratios for all six sections should be greater than the maximum fatigue ratios. All sections clearly exceed the maximum design ratio at each percentile from 50 to 99, thus validating the refined limiting criteria based on strains predicted from PerRoad for perpetual pavement design.

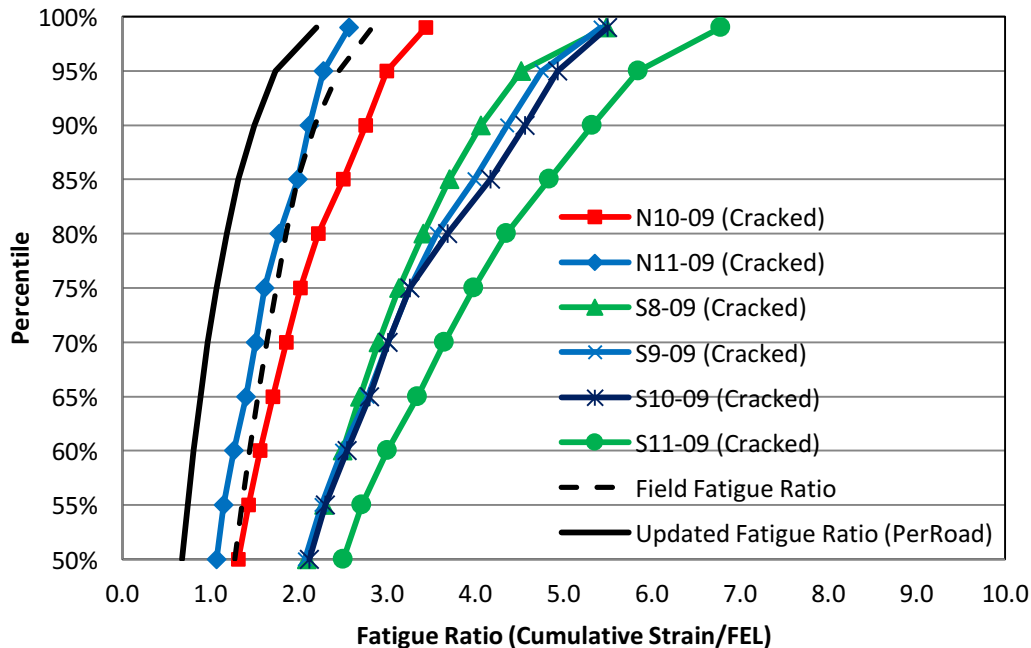


Figure 13 Validating Refined Maximum Fatigue Ratios Using 2009 Sections.

4 APPROXIMATE RANGES OF MAXIMUM DESIGN THICKNESSES

The limiting strain distribution presented in the previous section was used to develop approximate ranges of maximum design thicknesses for future design consideration. The analysis conducted in this study to develop approximate ranges of maximum design thicknesses was similar to that conducted in SHRP 2 Project R23 (22). Both analyses utilized the limiting strain approach via the PerRoad software (Version 3.5). The main difference between the two analyses was the criteria used to select the final thickness design as follows.

- In the SHRP 2 R23 analysis, the final AC thickness was selected if it would provide a damage ratio less than or equal to 0.1 at 10 years and 50 years of service life based on a fatigue endurance limit of 100 microstrain.
- In this study, the final thickness of AC layer was chosen based on the two criteria: the first criterion was to avoid the development of fatigue cracking, and the second criterion was to limit structural rutting occurred in subgrade.
 - The cumulative distribution of the calculated tensile strains at the bottom of the AC layer was lower than the limiting strain distribution listed in Table 10; and
 - 50% (or 50 percentile) of vertical strains calculated at the top of subgrade were below 200 microstrain.

Other inputs needed for the PerRoad simulations were selected as discussed below.

- One traffic level was simulated, which consisted of 100% of single axles weighing 20-22 kips. This represents a conservative traffic level within the legal load limits allowed in the U.S.
- The pavement structures (as simulated) had three layers, including an AC layer over a base layer over subgrade. Table 11 lists the inputs for each layer.

- For the AC layer, the moduli were influenced by the binder performance grade selected in the software and seasonal temperatures discussed below. The selected performance grade was a PG 64-34 for Minneapolis, a PG 70-22 for Phoenix, and a PG 64-22 for Baltimore, consistent with the SHRP2 R23 analysis. The AC thickness was designed to meet the design criteria.
- The base layer thickness was selected to be 6, 8, and 10 inches. Five base moduli were used in the simulations, including 30, 50, 100, 250, and 500 ksi.
- Three subgrade moduli were selected for the simulations, including 5, 10, and 20 ksi.
- The seasonal temperatures affecting the AC moduli used in this analysis are the same as those used in the SHRP 2 R23 analysis. In the SHRP 2 R23 study, trial runs were initially conducted for five cities (Minneapolis, MN; San Francisco, CA; Phoenix, AZ; Dallas, TX; and Baltimore, MD). However, it was found that the thickness values for San Francisco and Dallas fell within the range of thicknesses determined for the other cities and did not affect the averages significantly. Thus, the analysis conducted as part of this study included only three cities: Minneapolis, Phoenix, and Baltimore. Table 12 lists the seasonal temperatures for the three cities as reported in the SHRP 2 R23 report (22).

Table 11 Inputs for Pavement Structures Used in PerRoad Simulations

Layer	Modulus (psi)		Poisson's Ratio	Thickness	
	Input	Distribution (COV)	Input	Average	Distribution (COV)
AC	Varied based on binder and season	Log-normal (30%)	0.35	Varied	Normal (5%)
Base	30, 50, 100, 250, and 500 ksi	Log-normal (40%)	0.4	6, 8 and 10 in.	Normal (8%)
Subgrade	5, 10, and 20 ksi	Log-normal (50%)	0.45	Semi-infinite	Not applicable

For each pavement design simulation, the following step-by-step procedure was followed:

1. In PerRoad, open the Structural and Seasonal Information window.
 - a. Select the number of layers. For this analysis, the number of layers was three, including AC, aggregate base, and subgrade.
 - b. Input the seasonal information. For this analysis, the seasonal information, including the number of weeks and mean air temperature for each season, is shown in Table 12.
 - c. Select the performance grade (PG) of the binder used in the AC layer. For this analysis, a PG 64-34 was selected for Minneapolis, a PG 70-22 for Phoenix, and a PG 64-22 for Baltimore. Then, input Poisson's ratio, initial thickness, distribution, and COV for the AC layers as shown in Table 11.
 - d. Input the moduli, Poisson's ratios, distributions, and COVs for the base and subgrade as shown in Table 12.
 - e. Accept changes in this window.
2. Open the Loading Conditions window.

- a. Select 100% single axles weighing 20-22 kips to represent a conservative traffic level within the legal load limits allowed in the U.S.
 - b. Accept changes in this window.
 - c. Note: details of the traffic stream (two-way AADT, % trucks, % truck growth, etc.) are not input, as the strain due to a single axle load is of interest rather than the number of cycles to failure.
3. Perform PerRoad analysis to predict the tensile strain at the bottom of the layer and the vertical strain at the top of subgrade.
 4. Open the PerRoad output file in MS Excel and determine the cumulative tensile and vertical strain distributions.
 5. Check the distributions to determine:
 - a. If the cumulative tensile strain distribution at the bottom of the AC layer was lower than the limiting strain distribution listed in Table 10; and
 - b. If the 50 percentile of the vertical strain distribution at the top of subgrade were below 200 microstrain.
 6. If one of the above criteria did not pass, adjust AC thickness and repeat steps 4, 5, and 6 until all criteria are met.

Table 12 Seasonal Temperatures for Minneapolis, Phoenix, and Baltimore (22)

City	Overall Mean Temperature (°F)	Seasonal Information		
		Month	Week	Temperatures (°F)
Minneapolis	45°F	Winter Nov, Dec, Jan, Feb	17 weeks	21
		Spring Mar, Apr, May	13 weeks	45
		Summer June, July, Aug	13 weeks	70
		Fall Sept, Oct	9 weeks	56
Phoenix	70°F	Winter Dec, Jan, Feb	13 weeks	54
		Spring Mar, Apr, May	13 weeks	68
		Summer June, July, Aug, Sept	17 weeks	87
		Fall Oct, Nov	9 weeks	66
Baltimore	56°F	Winter Dec, Jan, Feb	13 weeks	35
		Spring Mar, Apr, May	13 weeks	54
		Summer June, July, Aug, Sept	17 weeks	74
		Fall Oct, Nov	9 weeks	53

Tables 13, 14, and 15 summarize results of the analysis and average thicknesses for 6-inch, 8-inch, and 10-inch bases, respectively, with resilient moduli of 30,000, 50,000, and 100,000 psi. Since the design scenarios simulated in this study used conservative inputs, the ranges of design thicknesses shown in these tables represent conservative design thicknesses encountered in future pavement design. Similar maximum thickness tables can be developed to represent state-specific climate, material, and subgrade conditions for use in conjunction with the agency-specific design procedure. When the thickness of a new or rehabilitated pavement design based on the agency-specific design methodology is greater than the maximum thickness, the agency may consider using the perpetual pavement design approach to optimize a design that can sustain the heaviest loads without being overly conservative.

Table 13 Ranges of Maximum AC Thicknesses for 6-inch Base (Mr = 30, 50, and 100 ksi)

Subgrade Mr (ksi)	Base Mr (ksi)	Calculated AC Thickness (in.)				Range of Maximum Thicknesses (in.)
		Minneapolis (PG 64-34)	Phoenix (PG 70-22)	Baltimore (PG 64-22)	Average	
5	30	12.5	15.5	14	14.0	12.5-15.5
5	50	12	15	14	13.7	12-15
5	100	12	14	13.5	13.2	12-14
10	30	10.5	14	12	12.2	10.5-14
10	50	10.5	13	12	11.8	10.5-13
10	100	10	12	11	11.0	10-12
20	30	9	12.5	10	10.5	9-12.5
20	50	8.5	12.5	9.5	10.2	8.5-12.5
20	100	8	12	9	9.7	8-12

Table 14 Ranges of Maximum AC Thicknesses for 8-Inch Base (Mr = 30, 50, and 100 ksi)

Subgrade Mr (ksi)	Base Mr (ksi)	Calculated AC Thickness (in.)				Range of Maximum Thicknesses (in.)
		Minneapolis (PG 64-34)	Phoenix (PG 70-22)	Baltimore (PG 64-22)	Average	
5	30	12.5	15	14	13.8	12.5-15
5	50	11.5	14.5	13.5	13.2	11.5-14.5
5	100	11	13	12.5	12.2	11-13
10	30	10.5	13	11.5	11.7	10.5-13
10	50	10	12	11.5	11.2	10-12
10	100	9	11	10.5	10.2	9-11
20	30	9	12.5	10.5	10.7	9-12.5
20	50	8.5	12	10	10.2	8.5-12
20	100	7.5	10.5	9	9.0	7.5-10.5

Table 15 Ranges of Maximum AC Thicknesses for 10-Inch Base (Mr = 30, 50, and 100 ksi)

Subgrade Mr (ksi)	Base Mr (ksi)	Calculated AC Thickness (in.)				Range of Maximum Thicknesses (in.)
		Minneapolis (PG 64-34)	Phoenix (PG 70-22)	Baltimore (PG 64-22)	Average	
5	30	12	14.5	13.5	13.3	12-14.5
5	50	11	13.5	12.5	12.3	11-13.5
5	100	10	12	11.5	11.2	10-12
10	30	10	12	11	11.0	10-12
10	50	9	11	10	10.0	9-11
10	100	8	10	9	9.0	8-10
20	30	8.5	11	10.5	10.0	8.5-11
20	50	7.5	10	9.5	9.0	7.5-10
20	100	6.5	9	8.5	8.0	6.5-9

A similar analysis was also conducted for stiff bases, such as rubblized or cracked and seated old portland cement concrete (PCC) pavements, with resilient moduli of 250,000 and 500,000 psi. Results of this analysis and average thicknesses are shown in Tables 16, 17, and 18 for 6-inch, 8-inch, and 10-inch bases, respectively. These results will require further evaluation and validation as the pavement sections used in the development and validation of the limiting strain criteria presented in this report did not include those that were constructed on rubblized or cracked and seated old PCC pavements. This is especially important for the very thin sections in Tables 17 and 18 where the base modulus is 500,000 psi. It is likely that these sections would suffer from reflective cracking not accounted for in perpetual pavement analysis.

Table 16 Ranges of Maximum AC Thicknesses for 6-inch Base (Mr = 250 and 500 ksi)

Subgrade Mr (ksi)	Base Mr (ksi)	Calculated AC Thickness (in.)				Range of Maximum Thicknesses (in.)
		Minneapolis (PG 64-34)	Phoenix (PG 70-22)	Baltimore (PG 64-22)	Average	
5	250	9.5	12	11	10.8	9.5-12
5	500	7.5	9.5	9	8.7	7.5-9.5
10	250	8	10	9.5	9.2	8-10
10	500	6	8	7	7.0	6-8
20	250	6.5	8	7.5	7.3	6.5-8
20	500	5	6	5.5	5.5	5-6

Table 17 Ranges of Maximum AC Thicknesses for 8-Inch Base (Mr = 250 and 500 ksi)

Subgrade Mr (ksi)	Base Mr (ksi)	Calculated AC Thickness (in.)				Range of Maximum Thicknesses (in.)
		Minneapolis (PG 64-34)	Phoenix (PG 70-22)	Baltimore (PG 64-22)	Average	
5	250	8.5	10.5	10	9.7	8.5-10.5
5	500	6	7.5	7	6.8	6-7.5
10	250	7	8.5	8	7.8	7-8.5
10	500	5	6	5.5	5.5	5-6
20	250	5.5	6.5	6	6.0	5.5-6.5
20	500	3	4	3.5	3.5	3-4

Table 18 Ranges of Maximum AC Thicknesses for 10-Inch Base (Mr = 250 and 500 ksi)

Subgrade Mr (ksi)	Base Mr (ksi)	Calculated AC Thickness (in.)				Range of Maximum Thicknesses (in.)
		Minneapolis (PG 64-34)	Phoenix (PG 70-22)	Baltimore (PG 64-22)	Average	
5	250	7	9	8	8.0	7-9
5	500	4.5	5.5	5.5	5.2	4.5-5.5
10	250	6	7	6.5	6.5	6-7
10	500	4.5	4	3.5	4.0	3.5-4.5
20	250	4	5	4.5	4.5	4-5
20	500	1.5	2	2	1.8	1.5-2

5 CONCLUSIONS

The objective of this study was to determine critical pavement design thresholds and approximate ranges of maximum thicknesses for flexible pavements. The study was divided into two tasks. The first task was to review literature pertaining to design thresholds and maximum thickness requirements for perpetual pavements. The second task was to evaluate and refine design thresholds and to determine maximum pavement thicknesses based on the information reviewed in Task 1 and through analyzing pavement response data from the fully instrumented pavement sections at the NCAT Pavement Test Track. Based on the results of the two tasks, the following conclusions are made.

- A perpetual pavement is designed to resist structural distresses, including bottom-up fatigue cracking and subgrade rutting. Historically, to prevent the initiation of bottom-up fatigue cracking, the strains at the bottom of the asphalt structure are kept below a design strain threshold, which is often the laboratory fatigue endurance limit (FEL) of the asphalt mixture used in the AC base layer. To prevent structural rutting, the vertical strain or stress at the top of the subgrade has been used as the limiting design parameter.
- The review of literature shows that the FEL has ranged in magnitudes from early estimates of 70 microstrain to more recent estimates of up to 200 microstrain. A value of 200 microstrain has been proposed for the vertical strain limit. In addition, past

perpetual pavement designs for high volume roadways had between 9 and 16 inches of AC depending on site-specific traffic, climate, material, and subgrade conditions.

- Studies have shown that the early estimated FEL of 70 microstrain was conservative. In addition, as shown in Table 9, the FELs of all the mixtures (including unmodified, modified, rich-bottom, and high RAP mixtures) analyzed in this study were higher than 70 microstrain.
- While a single limiting strain (i.e., 70 microstrain) or the FEL of the AC base layer have been proposed for designing long life pavements, neither were a good indicator of resistance to bottom-up fatigue cracking in the 2003 and 2006 structural test sections at the NCAT Pavement Test Track. Rather, the test sections that experienced bottom-up fatigue cracking had cumulative field-measured strain distributions clearly separated from those of test sections that did not crack. Based on this finding, a limiting cumulative strain distribution was developed based on field-measured strains for controlling bottom-up fatigue cracking in a past study.
- There are notable differences between field-measured strains at the bottom of the AC layer and tensile strains predicted by a structural pavement design program, such as PerRoad. As a result, the limiting strain distribution based on field-measured strains was adjusted to take such differences into account. The adjusted limiting cumulative strain distribution listed in Table 10 is proposed for use in place of a single FEL in future perpetual pavement design to control bottom-up fatigue cracking.
- Additionally, if the laboratory FEL of the AC base layer is available during the pavement design process, the fatigue ratios at incremental percentiles can be determined by dividing the corresponding cumulative strains predicted by the pavement design software by the FEL. These fatigue ratios can be compared with the limiting fatigue ratios listed in Table 10, which were also refined and validated in this study.
- The limiting strain distribution was used later in this study to develop approximate ranges of maximum design thicknesses for asphalt pavements. This analysis was similar to that conducted in Strategic Highway Research Program 2 Project R23. Both analyses used the limiting strain approach via the PerRoad software (Version 3.5). The main difference between the two analyses was the criteria used to select the final thickness design. The analysis was conducted based on a conservative traffic level within the legal load limits for various combinations of subgrade and base moduli in three climatic conditions to cover the potential ranges of maximum design thicknesses. The resulting approximate ranges of maximum design thicknesses for asphalt pavements are shown in Tables 13, 14, and 15 for base layers with resilient moduli of up to 100,000 psi. The maximum thickness has between 6.5 and 15.5 inches of AC depending on site-specific climate, material, and subgrade conditions.
- Additional analysis was also conducted for pavements constructed on stiff base layers, such as those built on rubblized and cracked and seated pavements, with resilient moduli of 250,000 and 500,000 psi. Results of this analysis are included in Tables 16, 17 and 18. These results will require further field evaluation and validation as the pavement sections used for developing and validating the limiting strain criteria in this study did not include those built on these stiff base layers, especially the very thin

sections in Tables 17 and 18 when the base modulus is 500,000 psi. It is likely that these thin sections would suffer from reflective cracking that is not accounted for in perpetual pavement analysis.

6 RECOMMENDATIONS

Based on the results and conclusions of this study, the following recommendations are made.

- The limiting cumulative strain distribution and fatigue ratios shown in Table 10 should be used in place of the conservative limiting strain of 70 microstrain or the laboratory FEL of the AC base layer in future perpetual pavement design.
 - These limiting values have been adjusted for the differences between field-measured and predicted tensile stains at the bottom of the AC. The adjusted limiting cumulative strain distribution was found to be the best indicator of how the structural test sections resisted bottom-up fatigue cracking at the NCAT Pavement Test Track.
- Tables 13, 14, and 15 show the ranges of maximum AC thicknesses for flexible pavement design. Similar tables can be developed based on the methodology presented in this report for each state that represents state-specific climate, material, and subgrade conditions.
- Further field evaluation and validation of the limiting strain criteria should be conducted to include pavement sections that were built on stiff base layers, such as those constructed on rubblized and cracked and sealed old concrete pavements. Additional thickness may be needed to resist reflective cracking not considered in perpetual pavement analysis.
- The maximum AC thickness tables can be used in conjunction with the agency-specific design procedure. When the thickness of a new or rehabilitated pavement designed based on the agency-specific design methodology is greater than the maximum thickness, the agency may use the perpetual pavement design approach to optimize the design that can sustain the heaviest loads to provide an indefinite structural life without being overly conservative.

7 REFERENCES

1. AASHTO. *AASHTO Guide for Design of Pavement Structures*, AASHTO, Washington, DC, 1993.
2. TRB. "Pavement Lessons Learned from the AASHO Road Test and Performance of the Interstate Highway System," *Transportation Research Circular Number E-C118*, Transportation Research Board, Washington, DC, 2007.
3. Newcomb, D., R. Willis, and D. Timm. *Perpetual Asphalt Pavements: A Synthesis*, APA, Lanham, MD, 2010.
4. Asphalt Pavement Alliance (APA). *Perpetual Pavements: A Synthesis*. APA 101, Lanham, MD, 2002.
5. Nunn, M., and B.W. Ferne. "Design and Assessment of Long-Life Pavements," *Transportation Research Circular No. 503*, Transportation Research Board, Washington, DC, 2001, pp. 32-49.
6. Thompson, M.R. and S.H. Carpenter. "Considering Hot-Mix-Asphalt Fatigue Endurance Limits in Full-Depth Mechanistic-Empirical Pavement Design," International Conference on Perpetual Pavements, Columbus, Ohio, 2006.
7. Bonaquist, R. "Developing a Plan for Validating an Endurance Limit for HMA Pavements," NCHRP 9-44, National Cooperative Highway Research Program, HMA Workshop Executive Summary, 2007.
8. Monismith, C. and D. McLean. "Structural Design Considerations," *Proceedings of the Association of Asphalt Paving Technologists*, Vol. 41, 1972.
9. Thompson, M.R. and S.H. Carpenter. "Perpetual Pavement Design: An Overview," International Conference on Perpetual Pavements, Columbus, Ohio, 2009.
10. Prowell, B., E.R. Brown, E.M. Anderson, J.S. Daniel, H. Von Quintus, S. Shen, S. Carpenter, S. Bhattacharjee and S. Maghsoodloo. *Validating the Fatigue Endurance Limit for Hot Mix Asphalt*, NCHRP Report 646, 2010.
11. Carpenter, S.H. and S. Shen. "Effect of Mixture Variables on the Fatigue Endurance Limit for Perpetual Pavement Design," International Conference on Perpetual Pavements, Columbus, Ohio, 2009.
12. Nishizawa, T., S. Shimeno, and M. Sekiguchi. "Fatigue Analysis of Asphalt Pavements with Thick Asphalt Mixture Layer," *Proceedings of the 8th International Conference on Asphalt Pavements*, Vol. 2, University of Washington, Seattle, WA, August 1997, pp. 969-976.
13. Wu, Z., Z. Q. Siddique, and A. J. Gisi. "Kansas Turnpike—An Example of Long Lasting Asphalt Pavement," *Proceedings International Symposium on Design and Construction of Long Lasting Asphalt Pavements*, National Center for Asphalt Technology, Auburn, AL, 2004, pp. 857-876.
14. Yang, Y., X. Gao, W. Lin, D.H. Timm, A.L. Priest, G.A. Huber, and D.A. Andrewski. "Perpetual Pavement Design in China," *Proceedings of International Conference on Perpetual Pavement*, Ohio University, 2006.
15. Von Quintus, H. "Application of the Endurance Limit Premise in Mechanistic-Empirical Based Pavement Design Procedures," International Conference on Perpetual Pavements, Columbus, Ohio, 2006.

16. Willis, J. R. and D. Timm. *Field-Based Stain Thresholds for Flexible Perpetual Pavement Designs*, NCAT Report 09-09, Auburn University, 2009.
17. Christopher, B., C. Schwartz, R. Boudreau. *Geotechnical Aspects of Pavements*, Report No. NHI-05-037, FHWA, U. S. Department of Transportation, Washington, D.C., 2006.
18. Monismith, C., J. Harvey, T. Bressette, C. Suszko, and J. St. Martin. "The I-710 Freeway Rehabilitation Project: Mix and Structural Section Design, Construction Considerations and Lessons Learned," *International Symposium on Design and Construction of Long Lasting Asphalt Pavements*, National Center for Asphalt Technology, Auburn, AL, 2004, pp. 217-262.
19. Walubita, L.F., W. Liu, T. Scullion and J. Leidy. "Modeling Perpetual Pavements Using the Flexible Pavement System Software," *Proceedings of the 87th Transportation Research Board Meeting*, Transportation Research Board, Washington, D.C., 2008.
20. Bejarano, M.O. and M. R. Thompson. "Subgrade Damage Approach for the Design of Airport Flexible Pavements," *Proceedings of the 2001 Airfield Pavement Specialty Conference: Advancing Airfield Pavements*, American Society of Civil Engineers. Washington, D.C., 2001, pp. 48-58.
21. Nunn, M. "Long-life Flexible Roads," *Proceedings of the 8th International Conference on Asphalt Pavements*, Vol. 1, University of Washington, Seattle, WA, August 1997, pp. 3–16.
22. Jackson, N., J. Mahoney, and J. Puccinelli. *Using Existing Pavement in Place and Achieving Long Life*, Final Report, SHRP 2 R23, TRB, Washington, D.C., 2012.
23. Rosenberger, C.E., T.J. Zurat and R.J. Cominsky. "A Practical Look at Pennsylvania's Bradford Bypass-A Perpetual Pavement," *Proceedings of International Conference on Perpetual Pavements*, Columbus, Ohio, 2006.
24. Lane, B., A.W. Brown and S. Tighe. "Perpetual Pavements: The Ontario Experiment," *Proceedings of International Conference on Perpetual Pavements*, Columbus, Ohio, 2006.
25. Sargand, S.M., I.S. Khoury, M.T. Romanello and J.L. Figueroa. "Seasonal and Load Response Instrumentation of the Way-30 Perpetual Pavements," *Proceedings of International Conference on Perpetual Pavements*, Columbus, Ohio, 2006.
26. Walubita, L.F., T. Scullion, J. Leidy and W. Lin. "A Review of the Texas Structural Design Criteria for Perpetual Pavement," *Proceedings of International Conference on Perpetual Pavements*, Columbus, Ohio, 2009.
27. Timm, D.H. and M.M. Robbins. "Perpetual Pavement Research at the NCAT Test Track," *Proceedings of the International Conference on Perpetual Pavements*, Columbus, Ohio, 2014.
28. Willis, J.R., D. Timm, A. Taylor, N. Tran, and A. Kvasnak. "Correlating Laboratory Fatigue Endurance Limits to Field-Measured Strains," *Journal of the Association of Asphalt Paving Technologists*, Volume 80, 2011, pp. 135-160.
29. Robbins, M., N. Tran, D. Timm, and J.R. Willis. "Adaptation and Validation of Stochastic Limiting Strain Distribution and Fatigue Ratio Concepts for Perpetual Pavement Design," Paper submitted to AAPT, 2014, pp. 32.

30. Robbins, M. and D. Timm. "Effects of Strain Pulse Durations on Tensile Strain in a Perpetual Pavement," *Proceedings of the International Conference on Perpetual Pavement*, Columbus, Ohio, 2009.
31. Timm, D., N. Tran, A. Taylor, M. Robbins, and R. Powell. "Evaluation of Mixture Performance and Structural Capacity of Pavements Utilizing Shell Thiopave[®]; Phase I: Mix Design, Laboratory Performance Evaluation and Structural Pavement Analysis and Design," *Report No. 09-05*, National Center for Asphalt Technology, Auburn University, 2009.
32. Timm, D.H. and A. PriestL. "Flexible Pavement Fatigue Cracking and Measured Strain Response at the NCAT Test Track," *Proceedings of the 87th Annual Meeting of the Transportation Research Board*, Transportation Research Board, National Research Council, Washington, D.C., 2008.
33. Timm, D.H., "Design, Construction and Instrumentation of the 2006 Test Track Structural Study," *Report No. 09-01*, National Center for Asphalt Technology, Auburn University, 2009.
34. Timm, D., M. Robbins, and J.R. Willis. "Characteristics of Two Perpetual Pavements at the NCAT Test Track," *Proceedings of the 3rd International Conference on Transportation Infrastructure*, Pisa, Italy, 2014.
35. Taylor, A. J. "Mechanistic Characterization of Resilient Moduli for Unbound Pavement Layer Materials," *M.S. Thesis*, Auburn University, 2008.